18th International Conference on the Application of Computer
Science and Mathematics in Architecture and Civil Engineering
K. Gürlebeck and C. Könke (eds.)
Weimar, Germany, 07–09 July 2009

MICROPLANE MODEL WITH INITIAL AND DAMAGE-INDUCED ANISOTROPY APPLIED TO TEXTILE-REINFORCED CONCRETE

R. Chudoba*, **A. Scholzen and J. Hegger**

**Institute of Structural Concrete*
RWTH Aachen University
Mies-van-der-Rohe-Str. 1, 52074 Aachen, Germany
E-mail: rostislav.chudoba@rwth-aachen.de

Keywords: Anisotropic damage model, Cementitious composites, Microplane model.

Abstract. *The presented material model reproduces the anisotropic characteristics of textile reinforced concrete in a smeared manner. This includes both the initial anisotropy introduced by the textile reinforcement, as well as the anisotropic damage evolution reflecting fine patterns of crack bridges. The model is based on the microplane approach. The direction-dependent representation of the material structure into oriented microplanes provides a flexible way to introduce the initial anisotropy. The microplanes oriented in a yarn direction are associated with modified damage laws that reflect the tension-stiffening effect due to the multiple cracking of the matrix along the yarn.*

1 INTRODUCTION

The highly heterogeneous material structure of textile reinforced concrete (TRC) leads to complex damage patterns including several mechanisms such as crack bridge initiation, debonding and filament rupture. It is important to include these micro-structural effects in the modeling strategy of TRC. On the other hand, for practical purposes, it is inevitable to use a smeared representation of the damage process. In particular, the model must allow an efficient calculation using a smeared crack approach and an implicit representation of the reinforcement.

The material model presented here uses a pragmatic meso-macro-scopic representation of the damage process that can be applied for damage patterns exhibiting sufficient degree of regularity (fine crack patterns). Such patterns occur for example in tensile zones of plates and shells. The present contribution will describe the applied theoretical approach and discuss the behavior of the model in elementary 2D loading conditions. The concept will be demonstrated on an example with non-reinforced concrete and on a reinforced specimen investigating different inclinations of the textile fabrics with respect to the loading direction.

The decomposition of the macroscopic behavior into different spatial directions is achieved by a spherical discretization of the material point into a set of oriented microplanes. It shall be emphasized here that the microplanes have neither the purpose nor the ambition of reflecting the microscopic layout of the material structure as interpreted by some authors. In spite of denoting them micro, their formulation still falls into the category of phenomenological models. The basic steps in the formulation of a microplane model are schematically depicted in Fig. 1 (a) for an early formulations of the microplane model including softening [1]:

- geometric projection of the macroscopic strain tensor to obtain the corresponding microplane strain vectors
- evaluation of constitutive laws at the microplane level
- an energetic homogenization of the microplane stress vectors to obtain the macroscopic stress tensor.

The energetic homogenization is based on the principle of virtual work stating that the work at the macroscopic level corresponds to the work at the microplane level [2]. Alternative formulations base their derivation on the equivalence of the Helmholtz free energy. It has been shown that for the basic microplane model as depicted in Fig. 1 (a) both approaches are equivalent and lead to the same formulations [3]. The involved integration at the microplane level can be evaluated numerically [4] as the weighted sum of all microplane contributions. Today a variety of microplane formulations exists. They differ in their focus and fields of application. The aim of the following section is to classify different models underlining the motivation behind their formulation, as well as the connected theoretical and numerical difficulties. From the mechanical point of view any material model should meet the following requirements:

- The model should be capable to reproduce the linear-elastic behavior for arbitrary values of Poisson's ratio, and
- should be thermodynamically consistent.
- From a practical point of view, the model should be able to reproduce available test data for different loading cases.

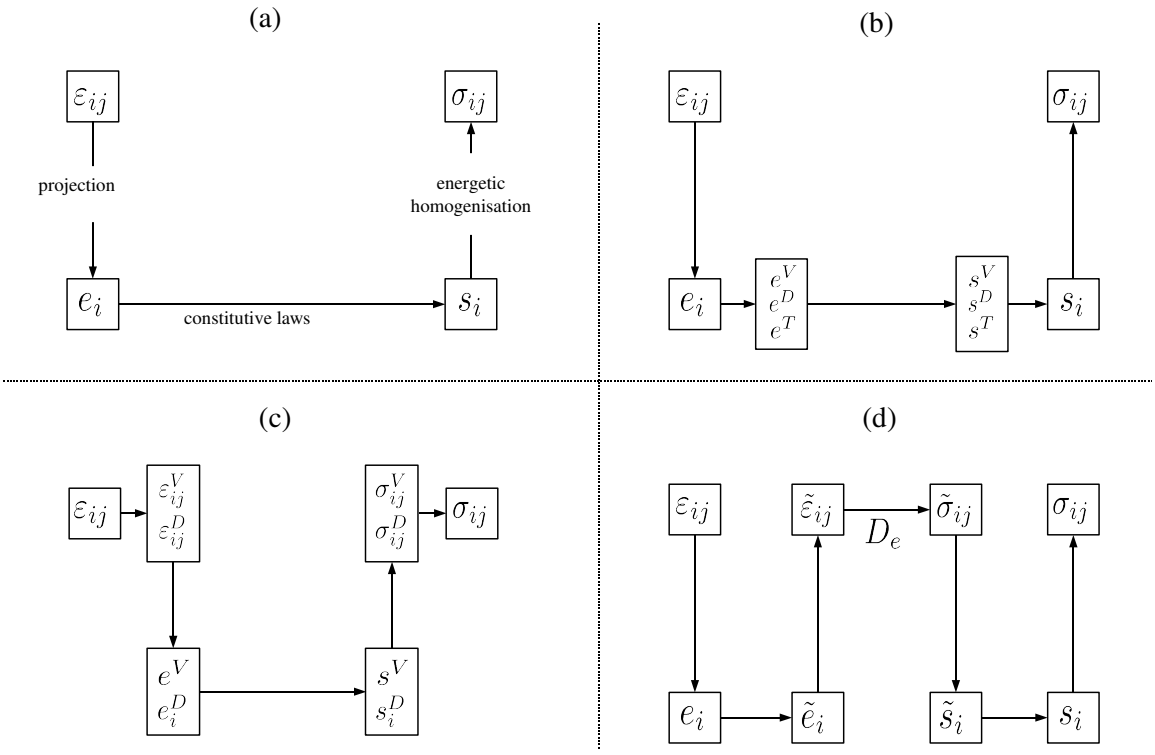

Figure 1: Classification of different types of microplane models: (a) basic principle of the microplane approach; (b) microplane formulation with split on the microplane level; (c) microplane formulation with split on the macroscopic level; (d) microplane formulation with explicit representation of the elasticity tensor.

The first microplane model as described in [5] was limited in its ability to reproduce the linear-elastic case and allowed only a certain range of values for the Poisson's ratio. This unnatural restriction was eliminated in the succeeding models [6] by splitting the microplane normal strains and stresses into a volumetric (e_V, s_V) and deviatoric part (e_D, s_D). The basic scheme of this class of microplane models is depicted in Fig. 1 (b). The shear component of the microplane strain/stress vectors ($\mathbf{e_i}$, $\mathbf{s_i}$) is denoted in the Figure by (e_T, s_T). The introduction of the split leads to the correct reproduction of arbitrary values of Poisson's ratio as well as a better behavior under triaxial compression. Despite of these improvements and convincing practical applicability of the model in terms of good fits and prediction of experimental behavior [7] for wide range of loading cases, this version of the model did not fulfill the requirement on thermodynamic consistency [3, 8]. On the other hand, if the split is introduced directly at the macroscopic level instead of the microplane level it leads to a thermodynamically consistent formulation. Further improvement of the microplane formulation within a thermodynamically sound framework has been achieved by combining the kinematic and static constraint. This extension was primarily motivated by the need to improve the model behavior in the softening regime for uniaxial tension [9].

In [10, 11] another thermodynamically consistent microplane formulation has been derived. In this particular formulation, the macroscopic strain tensor is split into a volumetric and a deviatoric part as depicted schematically in Fig. 1 (c). An alternative split based on spectral decomposition of the strain tensor was proposed in [12] for laminate composites. In both models

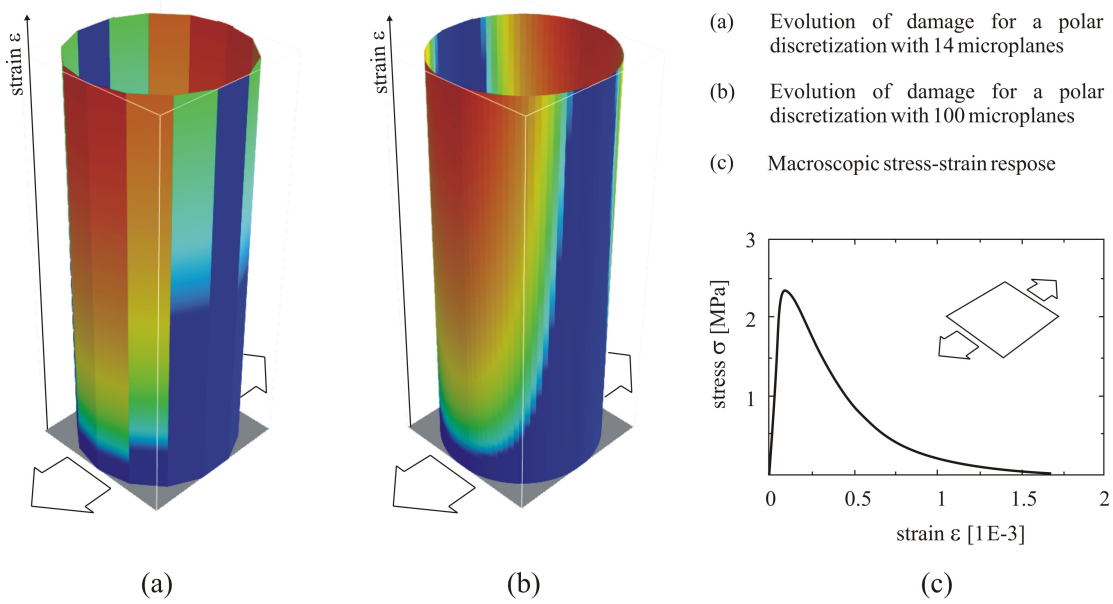

Figure 2: Anisotropic damage development for two different microplane resolutions of a single 2D material point loaded in tension.

the motivation behind the introduction of the split is to assign different constitutive laws to the decomposed parts in order to better capture the underlying failure mechanisms of the material in different loading situations. An alternative formulation that does not need the split was provided in [13]. The derived model is thermodynamically consistent and falls into the class of microplane models depicted in Fig. 1 (d). It is based on theoretical considerations devised in [2]. In contrast to the original microplane scheme in Fig. 1 (a) the connection between the effective macroscopic strain tensor and stress tensor is established explicitly using the elasticity tensor. This places this microplane model into the context of classical damage mechanics. For undamaged material the model can exactly reproduce the linear-elastic response. Furthermore, the Poison's effect is correctly reproduced for arbitrary values of the Poison's ratio.

2 DAMAGE INDUCED ANISOTROPY

In order to visualize the way how the microplane model represents the damage, Fig. 2 shows the response of a single 2D material point with initially isotropic, quasi-brittle behavior loaded in uniaxial tension. The longitudinal axis of the cylindric plot corresponds to the imposed macroscopic strain. The damage evolution obtained from the two-dimensional microplane formulation is depicted for two polar discretizations with 14 and 100 microplanes (cf. Fig. 2 (a) and (b)). The blue color corresponds to an undamaged material, i.e. $\phi = 1$, while the red color reflects complete material degradation in the direction of the corresponding microplane, i.e. $\phi = 0$. At the beginning of the loading process none of the microplanes exhibits damage as the material is still in the linear-elastic regime. With increasing macroscopic strain the damage initiates at the microplanes with positive (tensile) microplane strain. Due to the Poisson's effect the microplanes orthogonal to the loading direction exhibit negative (compressive) strains and remain undamaged even at large macroscopic strains. The overall macroscopic response is evaluated based on the damage parameters of all microplanes yielding a fourth order damage tensor.

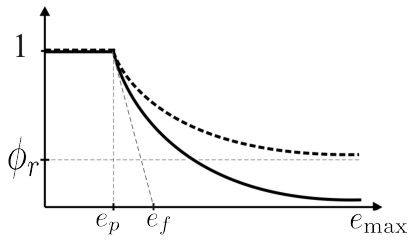

Figure 3: Damage function with different residual integrity for varying inclination angle.

This homogenization process exploits the principle of energy equivalence. The numerical integration involved shows sufficient accuracy already for a discretization with 14 microplanes, which has been used to obtain the depicted stress-strain-curve in Fig. 2 (c).

3 DAMAGE LAW WITH INITIAL ANISOTROPY

The microplane damage model introduced by [**?**] has been utilized to include the direction-dependent damage law specification. The explicit notion of microplane orientation makes the extension with direction-dependent parameters simple and transparent. Further, the geometrical and mechanical interpretation of the parameters can be easily established. In order to reflect the effect of reinforcement, the damage law corresponding to the reinforced direction must show a residual integrity. This has been implemented by introducing the variable ϕ_r into the damage law representing the horizontal asymptote at the desired level of residual integrity (cf. Fig 3).

$$\phi = f(e_{\max}) = \begin{cases} 1 & \text{if} \quad e_{\max} \leq e_{\mathrm{p}} \\ (1-\phi_r)\sqrt{\frac{e_{\mathrm{p}}}{e_{\max}}}\exp\left(-\frac{e_{\max}-e_{\mathrm{p}}}{e_{\mathrm{f}}-e_{\mathrm{p}}}\right)+\phi_r & \\ & \text{if} \quad e_{\max} \geq e_{\mathrm{p}} \end{cases} \tag{1}$$

In the example shown in Fig. 4 a value of $\phi_r = 0.40$ for the reinforced direction and a linear transition from the reinforced to the non-reinforced direction has been chosen to exemplify the computational procedure. The value of ϕ_r stays constant for the microplanes with an orientation that differs $\pm\pi/4$ from the reinforced direction. From that point on, ϕ_r decreases linearly to zero until the direction orthogonal to the reinforced direction is reached.

4 ELEMENTARY STUDY OF THE MODEL RESPONSE

In order to capture the discussed effects in a smeared approach on the macroscopic level the numerical model must be capable to reproduce the different behavior of the material in different directions. Fig. 4 exemplifies this for a TRC disk reinforced in one direction for different orientations of the reinforcement direction (indicated by the thick gray lines) with respect to the loading direction (indicated by the arrows). For the case of loading of the disk perpendicular to the reinforcement the damage of the material in this direction can be described by the use of a strain softening damage law. The same disk loaded in the reinforced direction exhibits multiple-cracking resulting in a pronounced tension stiffening effect in this direction. The corresponding damage law would have to show a residual integrity in order to reproduce the remaining stiffness of the cracked specimen.

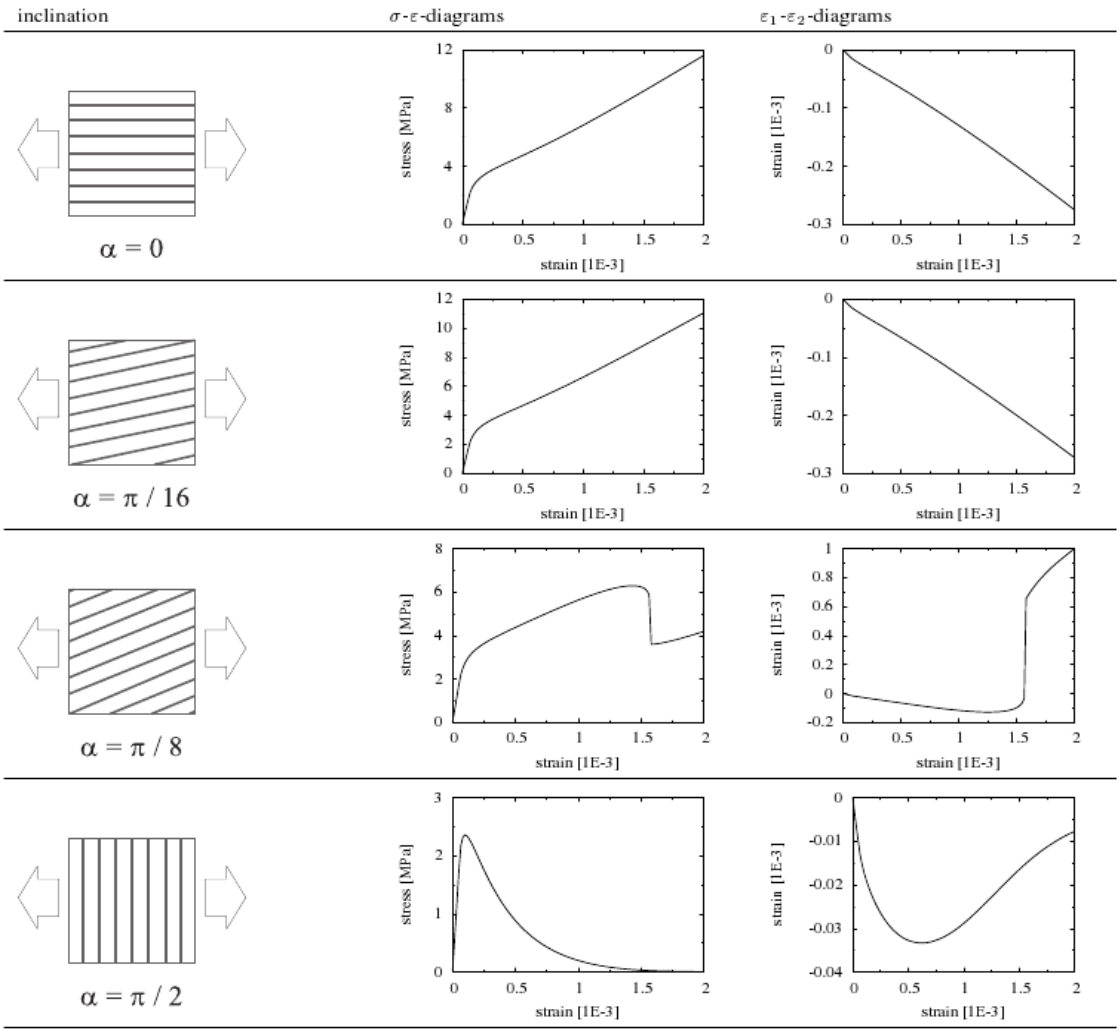

Figure 4: Simulated response of the composite for varied inclinations of the reinforcement; First column: reinforcement inclination; Second column: stress - strain response; Third column: development of the lateral strain versus control strain in the loading direction.

In the first column of Fig. 4 selected reinforcement inclinations at an angle α with respect to the loading direction are shown ($\alpha = 0$, $\alpha = \frac{\pi}{16} \approx 11°$, $\alpha = \frac{\pi}{8} \approx 22°$ and $\alpha = \frac{\pi}{2}$). For the case of loading in the direction of the reinforcement, i.e. $\alpha = 0$, a pronounced tension-stiffening effect is reproduced as can be seen in the corresponding stress-strain-diagram in Fig. 4. The principle strain ε_2 in the direction perpendicular to the loading direction (ε_1) is decreasing proportionally, i.e. develops linearly in the ε_1-ε_2-diagram. The strain ε_2 is induced by the Poisson's effect of the material and the negative values indicate that the material contracts in the 2-direction due to the strain in the 1-direction.

For a small inclination of the reinforcement, as shown for the case $\alpha = \frac{\pi}{16}$, the stress-strain-diagram and the corresponding ε_1-ε_2-diagram are almost identical to the described case of $\alpha = 0$. Only a slight decrease of the stiffness can be recognized in the stress-strain-diagram after the formation of cracks has finished. In both cases, $\alpha = 0$ and $\alpha = \frac{\pi}{16}$, no failure of the composite can be observed in the investigated strain range.

This is no longer the case for an inclination of the reinforcement of $\alpha = \frac{\pi}{8}$. Here, the

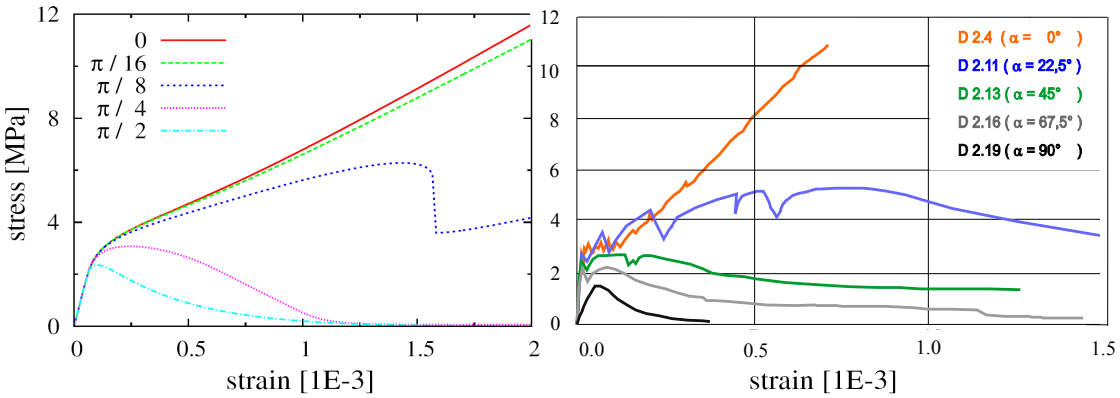

Figure 5: Qualitative comparison of the model response with the measured test data; Left: simulation with varied inclination of the reinforcement; Right: stress-strain response measured in tensile test on reinforced TRC specimens.

tension stiffening effect is less pronounced and the stiffness is further reduced. In contrast to the aforementioned cases the stiffness does not stay constant once the saturated crack state is reached but gradually decreases further which leads to the round shape of the corresponding stress-strain-curve. At a strain level of approximately 0.15% the stress drops rapidly. This would correspond to damage localization in the loaded specimen. In the corresponding ε_1-ε_2-diagram the failure of the composite coincides with change of the sign of the lateral strain ε_2 and its subsequent rapid growth. As a consequence, futher loading in the 1-direction results in lateral expansion of the disintegrated specimen in 2-direction. This can be interpreted as a localized damage in the direction perpendicular to the reinforcement. This does not correspond to the damage pattern occurring in the tensile test of a TRC specimen, where the localized crack bridges develop perpendicularly to the loading direction. Naturally, the loading with inclination $\alpha = \frac{\pi}{2}$ reproduces the response of a non-reinforced specimen.

5 CONCLUSIONS

The elementary study was performed with intuitively specified damage functions. Even for this rough estimate, the qualitative trends observed in the experiment could be reproduced as shown in Fig. 5. It must be emphasized that no fitting has been performed for this example. Systematic calibration methodology for the model using both experimental data and micro- and meso-mechanical models of the composite are currently being elaborated.

Summarizing, the model yields plausible results for initially anisotropic cementitous composites. The feasibility of the model has been demonstrated for the case of uniaxial loading with inclined reinforcement. Further adjustments of the introduced directional dependency of damage specification for TRC are necessary. In particular the kinematic behavior of the model during the localization process that must be adjusted in order to reflect the meso-level damage mechanisms occurring in the tested material.

REFERENCES

[1] Bazant, Z.P.; Gambarova, P.G. Crack shear in concrete: crack band microplane model. *J. Struct. Engng., ASCE*, 110, 2015-2036, 1984.

[2] Carol, I.; Bazant, Z.P. Damage and plasticity in microplane theory. *International Journal of Solids and Structures*, 34, 3807-3835, 1997.

[3] Carol, I.; Jirasek, M.; Bazant, Z. A thermodynamically consistent approach to microplane theory. PartI. Free energy and consistent microplane stresses. *Int. Journal of Solids and Structures*, 38, S. 2921-2931, 2001.

[4] Stroud, A. H. *Approximate calculation of multiple integrals*, Prentice-Hall, Englewood Cliffs, N. J., 1971

[5] Bazant, Z.P.; Oh, B.-H. Microplane model for progressive fracture of concrete and rock. *Journal of Engineering Mechanics, ASCE*, 111(4), 559-582, 1985.

[6] Bazant, Z.P.; Prat, P.C. Microplane model for brittle material. I: Theory. *Journal of Engineering Mechanics, ASCE*, 113(7), 1050-1064, 1987.

[7] Bazant, Z.P.; Caner, F.C.; Carol, I.; Adley, M.D.; Ankers, S.A. Microplane model M4 for concrete: I. Formulation with work conjugate deviatoric stress. *Journal of Engineering Mechanics*, 126(9), 944-953, 2000.

[8] Kuhl, E.; Steinmann, P.; Carol, I.; A thermodynamically consistent approach to microplane theory. PartII. Dissipation and inelastic constituive modelling. *Int. Journal of Solids and Structures*, 38, S. 2933-2952, 2001.

[9] Bazant, Z.P.; Caner, F.C. Microplane Model M5 with kinematic and static constraints for concrete fracture and anelasticity: I Theory. *Journal of Engineering Mechanics*, ASCE, 130 (1), 31-40, 2005.

[10] Kuhl, E.; Ramm, E Microplane modelling of cohesive frictional materials. *Eur. J. Mech. & Solids*, 19, S121-S143, 2000.

[11] Leukart, M.; Ramm, E. Identification and Interpretation of microplane material laws. *Journal of Engineering Mechanics*, ASCE, 132/3, 295-305, 2006.

[12] Cusatis, G.; Beghini, A.; Bazant, Z.P. Spectral Stiffness Microplane Model for QuasiBrittle Composite Laminates: I. Theory. *Journal of Applied Mechanics*, ASME, 75(2), 2008.

[13] Jirasek, M., Comments on microplane theory, *Mechanics of Quasibrittle Materials and Structures, Hermes Science Publications*, Paris, 55-77, 1999.